

## IMPLICATIONS OF THE LOW BINARY BLACK HOLE ALIGNED SPINS OBSERVED BY LIGO

KENTA HOTOKEZAKA<sup>1,2</sup> AND TSVI PIRAN<sup>2</sup>*draft v2*

## ABSTRACT

We explore the implications of the observed low spins aligned with the orbital axis in Advanced LIGO O1 run on binary black hole (BBH) merger scenarios in which the merging BBHs have evolved from field binaries. The coalescence time determines the initial orbital separation of BBHs. This, in turn, determines whether the stars are synchronized before collapse and hence determines their projected spins. Short coalescence times imply synchronization and large spins. Among known stellar objects, Wolf-Rayet (WR) stars seem the only progenitors consistent with the low aligned spins observed in LIGO's O1 provided that the orbital axis maintains its direction during the collapse. We calculate the spin distribution of BBH mergers in the local Universe and its redshift evolution for WR progenitors. Assuming that the BBH formation rate peaks around a redshift of  $\sim 2-3$ , we show that BBH mergers in the local Universe are dominated by low spin events. The high spin population starts to dominate at a redshift of  $\sim 0.5-1.5$ . WR stars are also progenitors of long Gamma-Ray Bursts (LGRBs) that take place at a comparable rate to BBH mergers. We discuss the possible connection between the two phenomena. Additionally, we show that hypothetical Population III star progenitors are also possible. Although WR and Population III progenitors are consistent with the current data, both models predict a non-vanishing fraction of high aligned spin BBH mergers. If those are not detected within the coming LIGO/Virgo runs, it will be unlikely that the observed BBHs formed via field binaries.

*Subject headings:* gravitational wave — black hole physics — gamma-ray burst: general — stars: black holes — stars: massive —

## 1. INTRODUCTION

The Advanced LIGO gravitational-wave (GW) detectors discovered binary black holes (BBHs) mergers. (Abbott et al. 2016c). The discovery has opened gravitational-wave astronomy of black holes. The GW measurements using a matched filter analysis provide us valuable information on the GW sources, e.g., the masses and spins of the BBHs. In addition, the luminosity distance or the cosmological redshift of the sources can also be measured, and thus, the event rate of BBH mergers is obtained. The resulting mass function of the primaries is consistent with the Salpeter initial mass function (Abbott et al. 2016b). Additionally, the inferred event rate is surprisingly high, about 0.1% of the current core-collapse supernova rate, suggesting that these are not the results of an obscure rare phenomenon. These facts motivate us to consider here the formation pathway of merging BBHs and their binary evolution and the impact on understanding astrophysical phenomena involving stellar mass black holes (see e.g. Abbott et al. 2016a and references therein).

The formation pathway of merging BBHs is one of the most intriguing mysteries that arose after the LIGO's discovery. One of the puzzles is how do so massive BBHs form in close binary systems. Such massive stellar progenitors are expected to evolve to giant stars whose stellar radii exceed significantly the semi-major axis that allows BBHs to merge within a Hubble time.

A possible scenario is one involving a dynamically-

unstable common envelope phase (see e.g. Belczynski et al. 2016). While a lot of works has been dedicated to this issue (see, e.g., Kruckow et al. 2016 for a recent work and Ivanova et al. 2013 and references therein), the outcome of common envelope phases is unknown. Other scenarios that avoid common envelope phases include chemically homogeneous evolution (Mandel & de Mink 2016), rapid-mass transfers (van den Heuvel et al. 2017), massive overcontact binaries (Marchant et al. 2016), and Population (Pop) III progenitors (Kinugawa et al. 2014; Inayoshi et al. 2017). We consider these scenarios here. We don't discuss here other scenarios that are not based on binary stellar evolution: a dynamical capture in dense stellar clusters (Rodriguez et al. 2016a; O'Leary et al. 2016), formation in galactic nuclei (Antonini & Rasio 2016; Bartos et al. 2017; Stone et al. 2017), and primordial BBHs (Sasaki et al. 2016; Bird et al. 2016; Blinnikov et al. 2016; Kashlinsky 2016).

A route to approach the progenitor scenario, on which we focus on in this paper, is to deriving the required conditions for the progenitors of BBH mergers from the observed parameters of the systems. This method allows us to avoid numerous uncertainties in modeling of the stellar evolution and the binary interaction. Kushnir et al. (2016) have recently pointed out that among the observable quantities the spin of merging BBHs parallel to the orbital axis seems to be the most useful to constrain the progenitor properties (see also Zaldarriaga et al. 2017). They have shown that the coalescence time of GW150914 is longer than 1 Gyr, if this merger arose from Wolf-Rayet (WR) stars in a field binary system. These discussions assume that natal kicks during the collapse don't change significantly the orbital angular momentum so that the aligned spin parameters are expected to have positive

<sup>1</sup> Center for Computational Astrophysics, Flatiron Institute, 162 5th Ave, New York, 10010, NY, USA

<sup>2</sup> Racah Institute of Physics, The Hebrew University of Jerusalem, Jerusalem 91904, Israel

TABLE 1  
PARAMETERS OF THE BBH MERGERS DETECTED DURING LIGO'S O1 RUN

Event	$m_1 [M_\odot]$	$m_2 [M_\odot]$	$m_{\text{tot}} [M_\odot]$	$\chi_{\text{eff}}$	Rate [ $\text{Gpc}^{-3} \text{yr}^{-1}$ ]
GW150914	$36.2^{+5.2}_{-3.8}$	$29.1^{+3.7}_{-4.4}$	$65.3^{+4.1}_{-3.4}$	$-0.06^{+0.14}_{-0.14}$	$3.4^{+8.6}_{-2.8}$
GW151226	$14.2^{+8.3}_{-3.7}$	$7.5^{+2.3}_{-2.3}$	$21.8^{+5.9}_{-1.7}$	$0.21^{+0.20}_{-0.10}$	$37^{+92}_{-31}$
LVT151012	$23^{+18}_{-6}$	$13^{+4}_{-5}$	$37^{+13}_{-4}$	$0.0^{+0.3}_{-0.2}$	$9.4^{+30.4}_{-8.7}$

The parameters are median values with 90% confidence intervals.  
The values are taken from Abbott et al. (2016b).

values. It is worthy noting that the aligned spin parameters measured by LIGO can be negative. Such negative values are naturally expected in the dynamical capture scenario (Rodriguez et al. 2016b).

The event rate of BBH mergers inferred by the LIGO's detections is similar to the rate of long Gamma-Ray Bursts (LGRBs) after the beaming correction with a reasonable value (Wanderman & Piran 2010). LGRBs are produced during the core collapse of massive stars. They are believed to form by a black hole surrounded by an accretion disk (Woosley 1993), which requires rapid rotation of the progenitor. These facts motivate us to explore the possibility that LGRBs are produced during the core collapse of massive stars in close binaries which eventually evolve to merging BBHs. In fact, such scenarios in which LGRBs arise from massive stars in close binaries have been already discussed (e.g. Podsiadlowski et al. 2004; Detmers et al. 2008; Woosley & Heger 2012).

In this paper, we consider the spins of BBH mergers for different types of progenitors and estimate the expected spin distribution and its redshift distribution. We briefly summarize the observed aligned spins of the BBH mergers detected in LIGO's O1 run in §2. We describe the spin and tidal synchronization of the progenitors in §3 and §4 and discuss different stellar models in §5. The possible connection between the BBH merger progenitors and LGRBs is discussed in §6. We show the spin distribution and its redshift evolution for the case of WR progenitors and Pop III progenitors in §7. We also discuss caveats of the spin argument in §8. We conclude our results in §9. In this paper, we use a  $\Lambda$ CDM cosmology with  $h = 0.7$ ,  $\Omega_\Lambda = 0.7$ , and  $\Omega_M = 0.3$ .

## 2. LIGO'S O1 GW DETECTIONS

*Mass function and Rate:* The masses and event rates of the three BBHs detected in LIGO's O1 run are summarized in Table 1. These event rates suggest that the primary mass function of BBH mergers is  $dR/dm_1 \propto m_1^{-\alpha}$ , where  $\alpha = 2.5^{+1.5}_{-1.6}$  and  $m_1$  is the mass of the primaries. The total BBH merger rate density is then  $99^{+138}_{-70} \text{Gpc}^{-3} \text{yr}^{-1}$  for  $\alpha = 2.35$  and  $m_{1,\text{min}} = 5M_\odot$ , where this minimal mass is based on the observed population of these mergers (Abbott et al. 2016b). This choice is consistent with observations of Galactic black holes (see, e.g. Özel et al. 2010; Farr et al. 2011). Note that the total event rate is sensitive to the choice of  $m_{1,\text{min}}$  that is still uncertain. If we take the secondary mass of GW151226,  $7.5M_\odot$ , as the minimal black hole mass in BBH mergers, the total event rate decreases to  $57 \text{Gpc}^{-3} \text{yr}^{-1}$ .

This primary mass function is consistent with the Salpeter initial mass function of local stars (Abbott et al. 2016b), suggesting that these BBHs may originate from

binary stellar objects. In addition, the event rate is similar to that of LGRBs, which are thought to be associated with black hole formations. In §7 and §8, we will discuss a scenario motivated by this similarity in which LGRBs are produced at the core collapse of massive stars in binary systems that eventually evolve to BBH mergers.

*Spin parameters:* The spin angular momentum of the merging BBHs can be inferred from the gravitational-wave signals. The effective spin parameter  $\chi_{\text{eff}}$  is a mass-weighted mean spin angular momentum of the two black holes parallel to the orbital angular momentum:

$$\chi_{\text{eff}} \equiv \frac{m_1}{m_{\text{tot}}}(\vec{s}_1 \cdot \hat{L}) + \frac{m_2}{m_{\text{tot}}}(\vec{s}_2 \cdot \hat{L}), \quad (1)$$

where  $m_2$  is the secondary mass,  $m_{\text{tot}} = m_1 + m_2$ ,  $\vec{s}_1$  and  $\vec{s}_2$  are the specific spin angular momenta of the primary and secondary normalized by the speed of light  $c$ , gravitational constant  $G$ , and mass of each component, and  $\hat{L}$  is the unit vector of the orbital angular momentum. This is well constrained as compared with the individual component spins that are not. The measured values are shown in Table 1.  $-1 \leq \chi_{\text{eff}} \leq 1$ , where the lower limit arises when both black holes' spins are maximal and anti-aligned to the orbital axis and the upper limit when both are maximal and aligned. If one of the black holes' spins is maximal and aligned and the other one is not we expect  $\chi_{\text{eff}} \approx 0.5$  for equal mass BBHs. The observed values of  $\chi_{\text{eff}}$  clearly exclude rapidly rotating synchronized progenitors whose spin axis is parallel to the orbital axis. As pointed out by Kushnir et al. (2016); Rodriguez et al. (2016b), these measured effective spin parameters depend sensitively on the evolutionary path of progenitors of BBHs and provide important constraints on the origin of BBH mergers. We focus on the spin evolution of the BBH progenitors in the rest of the paper. Note that the error range of the observed  $\chi_{\text{eff}}$  of GW151226 does not exclude the possibility that the spin parameter of the secondary is of order unity if the primary's spin is much smaller than unity.

## 3. BINARY BLACK HOLE PROGENITORS' SPIN

A binary system with stellar masses  $m_1$  and  $m_2$  at a semi-major axis  $a$  inspirals in due to gravitational-wave radiation. The time until the coalescence,  $t_c$ , is (Peters 1964):

$$t_c = \frac{5}{256} \frac{a}{c} \frac{c^2 a}{G m_1} \frac{c^2 a}{G m_2} \frac{c^2 a}{G m_{\text{tot}}} \quad (2)$$

$$\approx 10 q^2 \left( \frac{2}{1+q} \right) \left( \frac{a}{44 R_\odot} \right)^4 \left( \frac{m_2}{30 M_\odot} \right)^{-3} \text{Gyr},$$

where  $q \equiv m_2/m_1$ . For binaries with  $t_c = 10$  Gyr, the corresponding orbital period is:  $P_{\text{orb}} \approx 4.4 \text{ day } (a/44R_\odot)^{2/3} (m_{\text{tot}}/60M_\odot)^{-1/2}$ . Note that, for simplicity, we assume circular orbits here and elsewhere. Such orbits are expected within most binary evolution scenarios (see, e.g., Zahn 1977 for the orbital circularization due to the tidal torque), as long as natal kicks at the black hole formation are not significant.

The stellar radius cannot exceed the Roche limit. The Roche limit of the secondary (Eggleton 1983) is  $R_{\text{RL}} \approx 0.49q^{2/3}a/[0.6q^{2/3} + \ln(1 + q^{1/3})]$ . For equal mass binaries:  $R_{\text{RL}} \approx 0.38a$ . We denote hereafter the primary (secondary) as the first (second) star evolving to core collapse. Requiring  $R_2 < R_{\text{RL}}$  and a coalescence time less than a Hubble time yields:

$$R_2 \lesssim 17R_\odot (m_2/30M_\odot)^{3/4}, \quad (3)$$

where  $R_2$  is the stellar radius of the secondary and we have assumed  $q = 1$ . In the rest of the paper, we consider massive stars that satisfy this condition.

Clearly if the stellar spin just before the collapse is larger than the maximal Kerr black hole spin, some mass and angular momentum will be shed out and the formed black hole will be a maximal Kerr. Otherwise, the spin angular momentum of the black hole equals to its progenitor's one (see, e.g., Barkov & Komissarov 2010, and also Sekiguchi & Shibata 2011; O'Connor & Ott 2011 for numerical studies). A critical question is whether the star is synchronized (tidally locked) with the orbital motion before the collapse. We characterize this by a synchronization parameter  $x_s$ , e.g.,  $x_s = 1$  and 0 correspond to a star tidally synchronized with the orbital motion and a non-rotating star, respectively. We don't expect negative values of  $x_s$  (counter rotating stars) and values larger than unity.

If there are no significant mass and angular momentum losses from the system during the collapse the spin of the secondary black hole is characterized by its stellar mass, radius, and semi-major axis:

$$J_2 = x_s I_2 \Omega_{\text{orb}}, = x_s \epsilon m_2 R_2^2 \left( \frac{G m_{\text{tot}}}{a^3} \right)^{1/2}, \quad (4)$$

where  $\epsilon$  characterizes the star's moment of inertia  $I_2 \equiv \epsilon m_2 R_2^2$ . Here and in the following, we consider, for simplicity, rigidly rotating stars. The spin parameter is then

$$\begin{aligned} \chi_2 &\equiv \frac{J_2}{m_2 r_{g,2} c}, \\ &= x_s \epsilon \left( \frac{R_2}{r_{g,2}} \right)^{1/2} \left( \frac{R_2}{a} \right)^{3/2} \left( \frac{m_{\text{tot}}}{m_2} \right)^{1/2} \approx x_s \left( \frac{\epsilon}{0.075} \right) \\ &\times \left( \frac{R_2}{4.7R_\odot} \right)^2 \left( \frac{a}{44R_\odot} \right)^{-3/2} \left( \frac{m_{\text{tot}}}{2m_2} \right)^{1/2} \left( \frac{m_2}{30M_\odot} \right)^{-1/2}, \end{aligned} \quad (5)$$

where  $r_{g,2} \equiv Gm_2/c^2$ . The normalizations of  $R_2$  and  $a$  were chosen so that the spin parameter is unity for  $x_s = 1$  and the merger takes place on a time scale of 10 Gyr.

The spin parameter can be directly related to the

merger time scale:

$$\begin{aligned} \chi_2 &\approx x_s q^{1/4} \left( \frac{1+q}{2} \right)^{1/8} \left( \frac{\epsilon}{0.075} \right) \\ &\times \left( \frac{t_c}{10 \text{ Gyr}} \right)^{-3/8} \left( \frac{R_2}{4.7R_\odot} \right)^2 \left( \frac{m_2}{30M_\odot} \right)^{-13/8}. \end{aligned} \quad (6)$$

#### 4. SYNCHRONIZATION

In close binary systems, the tidal torque on the stars forces them to reach an equilibrium state, where the stellar rotation is synchronized with the orbital motion. The synchronization timescale of a star with a radiative envelope and a convective core can be estimated as

$$\begin{aligned} t_{\text{syn}} &\approx 0.07 \text{ Myr } q^{-2} \left( \frac{1+q}{2} \right)^{-5/6} \left( \frac{\epsilon}{0.075} \right) \left( \frac{R}{14R_\odot} \right)^{-7} \\ &\times \left( \frac{M}{30M_\odot} \right)^{-1/2} \left( \frac{a}{44R_\odot} \right)^{17/2} \left( \frac{E_2}{10^{-6}} \right)^{-1}, \end{aligned} \quad (7)$$

where  $E_2$  is a dimensionless quantity depending on the stellar structure introduced by Zahn (1975).  $E_2$  is  $\sim 10^{-7}$ – $10^{-4}$  for massive main sequence stars and WR stars (Zahn 1975; Kushnir et al. 2017). It may be smaller for blue supergiants. For WR progenitors, Kushnir et al. (2016) derive a useful form of Eq. (7) as:

$$t_{\text{syn}} \approx 10 \text{ Myr } q^{-1/8} \left( \frac{1+q}{2q} \right)^{31/24} \left( \frac{t_c}{1 \text{ Gyr}} \right)^{17/8}. \quad (8)$$

We will use this form for WR progenitors in §7.

If the synchronization time is much shorter than other timescales, e.g., the stellar lifetime and the wind angular-momentum loss timescale, the star is synchronized with the orbital motion, i.e.,  $x_s = 1$ . On the contrary, if the synchronization time is much longer than the others, the stellar spin parameter decreases with time due to the wind loss from the initial value.

If the synchronization timescale is comparable to the stellar lifetime or the wind timescale, which is the case for WR progenitors, one needs to solve the time evolution of the synchronization parameter. In the following we estimate the spin evolution of close binary WR stars using the formulation of Kushnir et al. (2016), that takes into account the tidal synchronization, wind mass loss, and the stellar lifetime. Given an initial value  $x_{s,i}$  at the beginning of the WR phase, the synchronization parameter evolves as:

$$\frac{dx_s}{d\tau} = \frac{t_w}{t_{\text{syn}}} (1 - x_s)^{8/3} - x_s, \quad (9)$$

where  $t_w$  is the time scale of spin angular momentum loss and  $\tau = t/t_w$ . The solution approaches to an equilibrium value,  $x_{s,\text{eq}}$ , at late times:

$$\frac{t_w}{t_{\text{syn}}} (1 - x_{s,\text{eq}})^{8/3} = x_{s,\text{eq}}. \quad (10)$$

Note, however, that  $t$  cannot exceed the stellar lifetime  $t_*$ . The approximate solutions at  $t_*$  are summarized in Kushnir et al. (2016) for different parameter regions.

If the timescale of the angular momentum loss due to the wind is longer than the stellar lifetime, the synchronization parameter of a star at the end of its lifetime,  $x_{s,f}$ , can be estimated as:

$$x_{s,f} \approx \begin{cases} \max(1 - t_*/t_w, x_{s,\text{eq}}) & \text{for } x_{s,i} = 1, \\ \min(t_w/t_{\text{syn}}, x_{s,\text{eq}}) & \text{for } x_{s,i} = 0. \end{cases} \quad (11)$$

In order to estimate the synchronization parameter of the WR stars at the end of their life in §7, we will use the above solutions with the following parameters:  $t_w = 1$  Myr and  $t_{\text{WR}} = 0.3$  Myr (Langer et al. 1994; Meynet & Maeder 2003, 2005). Using the synchronization parameter we calculate the spin parameter of the individual black holes for a given mass, radius, and coalescence time  $t_c$ .

For the wind angular momentum losses, we assume that isotropic winds remove the outermost spherical shell of a star with spin angular momentum of  $2M_s R_*^2 \Omega_*/3$ , where  $M_s$  is the mass of the shell,  $R_*$  and  $\Omega_*$  are the stellar radius and spin angular frequency. In this description,  $t_w \approx 1$  Myr corresponds to a mass loss rate of  $\sim 10^{-5.5} M_\odot/\text{yr}$ . Note that, however, the efficiency of the spin angular momentum loss due to winds can be either lower or higher. For instance, winds may have anisotropic structures due to a fast stellar rotation, that removes less spin angular momentum (Meynet & Maeder 2007). On the contrary, magnetic winds carry out spin angular momentum more efficiently depending on the field strength (e.g. Ud-Doula et al. 2009). Note also that a significant mass loss from a binary increases the semi-major axis. However, because the spin angular momentum is more efficiently lost from the stellar surface for rigidly rotating stars, the mass loss timescale is  $\sim 10t_w(0.075/\epsilon)$  for the isotropic winds. With the parameters we consider here, this effect on the semi-major axis is negligible.

The gravitational-wave measurements are quite insensitive to the spin components perpendicular to the orbital axis as the observed  $\chi_{\text{eff}}$  measures only the spin parallel to the orbital axis. In the following discussion, we assume that the misalignments of the BBHs' spin axes to the orbital axis are negligible, and hence, the synchronization parameters cannot be negative. This assumption is valid as long as the progenitor binaries do not receive significant kicks at the black hole formation. As we will discuss in §8, such kicks are unlikely when black holes form. On the contrary, the dynamical capture scenario of merging BBH formation naturally predicts that a half of mergers have negative values of  $\chi_{\text{eff}}$ . Note that the measured effective spin parameters of GW150914 and LVT151012 allow negative values within errors. Therefore the discovery of BBHs with a negative  $\chi_{\text{eff}}$  will have a significant impact on the understanding of the formation scenarios and the kick at the black hole formation (Rodriguez et al. 2016b).

## 5. SYNCHRONIZATION FOR DIFFERENT STELLAR MODELS

As the stellar radius and resulting black hole's spin are tightly connected, the spin measurements strongly constrain the possible progenitors of the observed BBH mergers. Population synthesis calculations considering the stellar evolution and the binary interactions are often

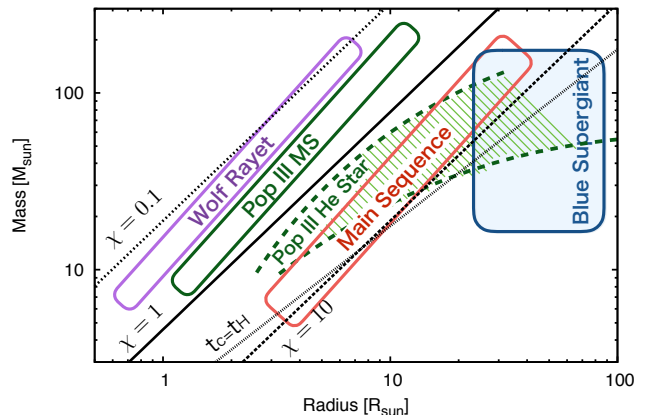


FIG. 1.— Mass - radius relations of different stellar models. The diagonal (dotted, solid and short-dashed black) lines depict the resulting black hole dimensionless spin for these masses and radii assuming that the star is synchronized at a semi-major axis where the coalescence time is a Hubble time. Also shown as a diagonal line labeled by  $t_c = t_H$  is the stellar radius limited by the Roche limit. Stars in the right side of this line cannot exist in a binary system whose coalescence time is less than a Hubble time. The curves are drawn for a mass ratio,  $q$ , of unity. One can clearly see that most models will result in  $\chi$  values much larger than unity.

used to estimate the rate, mass, and spin distribution of compact binary mergers and to discuss their progenitors. Here we take a different approach. We don't discuss the binary evolution. Instead we focus on the the observed low aligned spins and examine their implications on the stellar progenitor just before its core collapse to a black hole.

We consider known types of massive stellar objects and hypothetical Pop III stars. The BBH mergers event rate suggests that, if they form via binary stellar evolution, there are  $\sim 10$  or less such progenitors in the Galaxy (using  $0.01 \text{ Mpc}^{-3}$  as the number density of the Milky-Way size galaxies and a stellar lifetime of 1 Myr). With such a small number it is possible and even likely that we have not identified these objects in the Galaxy. It is interesting to note, in passing, that Gaia might be able to identify these binaries as they involve the most massive stars and hence most luminous stars.

Figure 1 depicts the mass - radius relation of the different stellar models. Three diagonal lines depict the spin parameters of these stars  $\chi = 0.1$ , 1, and 10 (see Eq. 5), if they are synchronized at the semi-major axis for which a binary coalesces in a Hubble time. Also shown as a diagonal line is the critical stellar radius that exceeds the Roche limit in a binary system that coalesces in a Hubble time (see Eq. 3). Figure 2 shows the relation between the effective spin parameters of different stellar models with the observed values from Abbott et al. (2016b). Here we assume a mass ratio  $q = 1$ , the single (double) synchronization means that one of (both) the black holes in a BBH is formed from a synchronized star. When comparing the models with the measured values of  $\chi_{\text{eff}}$  we further assume that the spin axes of BBHs are aligned with the orbital axis (see §8 for caveats).

For a given stellar model and a given coalescence time the spin parameter of the synchronized progenitors de-

depends rather weakly on the stellar mass. More specifically, the spin parameter behaves as  $\chi \propto m^{-0.225}$  for  $R \propto m^{0.7}$ , which is a typical dependence of the radius of massive stars on the mass (Tout et al. 1996; Kushnir et al. 2016). Thus the spin parameter reflects the time delay between the formation and the coalescence irrespective of the BBH mass.

(i) *Main-sequence stars*: While we don't expect a main-sequence star to collapse directly to a black hole, we begin with main-sequence binaries and show that these are ruled out. Main-sequence stars with masses  $\gtrsim 10M_{\odot}$  can exist in a binary system with  $t_c = 10$  Gyr without exceeding its Roche limit.

Massive main-sequence stars in close binaries with  $t_c \lesssim 10$  Gyr are synchronized on timescales much shorter than their lifetime (see Eq. 7, where we used the stellar structure of main-sequence stars at the median point of their lifetime; Tout et al. 1996; Hurley et al. 2000). Thus, main-sequence stars are tidally synchronized. In fact, Galactic O-star binaries with orbital periods  $\lesssim 10$  days are likely tidally synchronized (Ramírez-Agudelo et al. 2015). The spin parameter of such main-sequence stars always exceeds unity. Therefore we can rule out the possibility that the BBHs detected in LIGO's O1 run have been formed directly from the collapse of main-sequence stars.

If the BBHs formed via binary evolution beginning with two main-sequence stars, then in order to reduce the spin parameter significantly the progenitors must have experienced either a significant mass loss carrying out most of their spin angular momentum (more than 95%) or a significant decrease in the semi-major axis during their evolution. The former may occur due to a wind or to mass transfer during the late phase and the latter may occur during a common envelope phase. The natural outcomes of these processes are WR stars, which we discuss later in this and the following sections. This conclusion seems to be consistent with stellar and binary evolution models (e.g. Belczynski et al. 2016).

(ii) *Red supergiant stars* are late massive stars with an extended hydrogen envelope, in which the convection is deeply developed. These stars are located around the Hayashi line in HR diagrams, where the corresponding temperatures are around 3000–4000 K. Red supergiants have high luminosities and cool effective temperatures, implying that they have large radii of 100 to  $10^3 R_{\odot}$ . BBHs arising from such wide binaries never merge within a Hubble time so that we can robustly exclude the scenario that red supergiants are the progenitors of merging BBHs just prior to the core collapse.

(iii) *Blue-supergiant stars* are massive stars at their late phase with a hydrogen radiative envelope (see, e.g., Langer et al. 1994; Meynet et al. 2011; Hirschi et al. 2004). Their radii can be 10 –  $30R_{\odot}$ , corresponding to high effective temperatures, and can be smaller than the Roche limit of a binary with a coalescence time of 10 Gyr. The spin parameter of blue supergiants is always much larger than unity if they are synchronized. Therefore, these stars are unlikely progenitors of LIGO's O1 events. However, the synchronization time is quite sensitive to the structure of the envelope and hence it is somewhat uncertain. We will address this issue in a separate work.

(iv) *WR stars* are late phase massive stars that have lost most of their hydrogen envelope (see, e.g., Langer

et al. 1994; Meynet & Maeder 2003, 2005). Importantly, a few WR–black hole binaries that are likely to evolve to merging BBHs have been observed in nearby galaxies (see Prestwich et al. 2007; Silverman & Filippenko 2008 for IC10 X-1, Carpano et al. 2007; Crowther et al. 2010 for NGC 300 X-1, Bulik et al. 2011 for the inferred BBH merger rate, Liu et al. 2013 for M 101 ULX-1, and see also Esposito et al. 2015 for more candidates). Because of the lack of the hydrogen envelope, the stellar radius is small. It is related to the mass as  $R \approx R_{\odot}(M/10M_{\odot})^{0.7}$  (Kushnir et al. 2016). The spin parameters of BBHs formed via synchronized WR stars are shown in Fig. 2. For systems with  $t_c \sim 10$  Gyr, the spin parameters can be as small as 0.1. These values are consistent with the measured effective spin parameters of the LIGO's O1 events. However, based on Eq. (8), WR stars are so compact that WR stars in binaries with  $t_c \gtrsim 1$  Gyr are not tidally synchronized within their lifetime. We will discuss further the spin parameters of WR progenitors in §7.

(v) *Population III stars* have formed from pristine gas. They are typically massive stars with twenty to a few hundreds  $M_{\odot}$  (Hosokawa et al. 2011; Hirano et al. 2014). Their radii are much smaller than those of normal main-sequence stars because the core, that lacks metals, needs to be compact in order to produce sufficient heats through nuclear burning to support the stellar mass (e.g. Omukai & Palla 2003). Since Pop III stars form only in the very early Universe around a redshift of  $\sim 10$  (e.g. de Souza et al. 2011), BBH mergers at the local Universe that originate from Pop III stars have a coalescence time of  $\sim 10$  Gyr. Using Pop III stellar structure calculated by Marigo et al. (2001) we find that even though Pop III stars are small, if they are synchronized, the spin parameters of BBH mergers in the local Universe are between 0.2 and 0.6 (see Fig. 4). However, the synchronization time of such systems is  $\sim 10$  Myr, which is comparable to their lifetime, so that Pop III stars in such binaries may not be fully synchronized. Therefore Pop III stars can be the progenitors of LIGO's O1 events.

The spin parameter of Pop III stars exceeds unity if the synchronization occurs during the He-burning phase (see Fig. 1). However, these stars have a convective core with a small radius and a shorter lifetime, thereby synchronization probably does not occur during this Pop III He burning phase. Furthermore, massive Pop III He stars exceed their Roche limit (see Fig. 1). Therefore some fraction of the spin angular momentum may be removed due to mass transfer in this phase.

## 6. LONG GRBS AND BBH MERGERS

LGRBs arise from the core collapse of massive stars. Supernovae associated with LGRBs are type Ibc, suggesting that the progenitors are stripped stars, e.g., WR stars. The progenitors' radii can be estimated from the properties of the prompt emissions as follows. The plateau in  $dN_{\text{GRB}}/dT_{90}$ , where  $N_{\text{GRB}}$  is the number of observed LGRBs and  $T_{90}$  is the duration of prompt emission containing 90% of its gamma-ray fluence, indicates that the typical jet break-out time from the stellar surface is  $\sim 15$  s (Bromberg et al. 2012). This break-out time is related to the progenitor's parameters as (Bromberg et al.

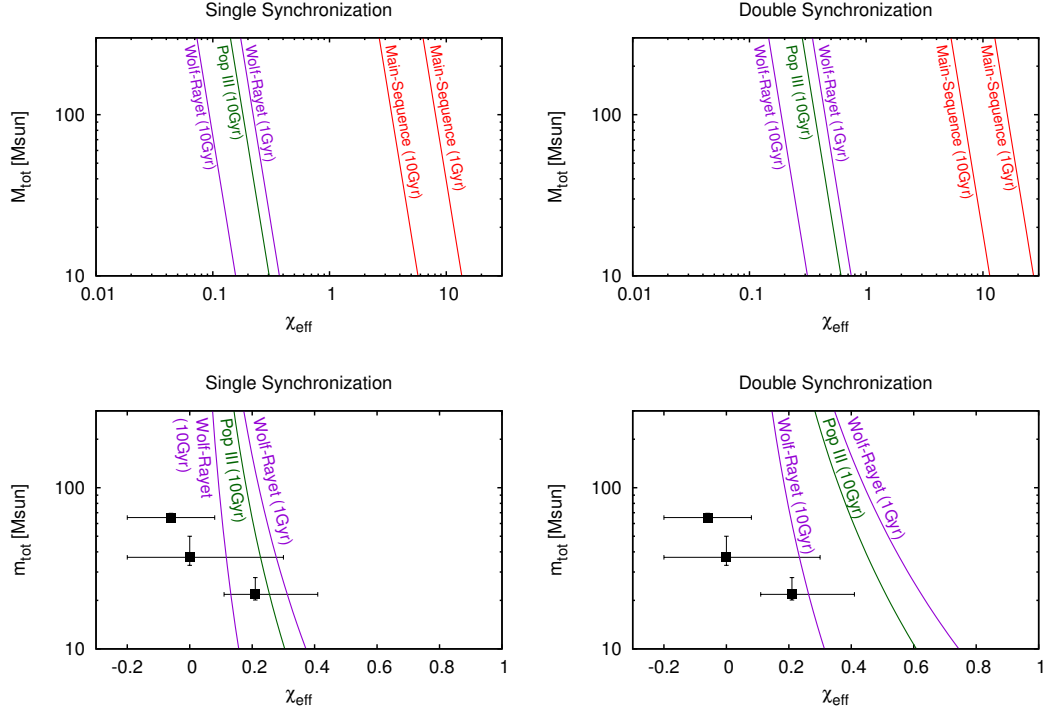


FIG. 2.— The spin and total mass of binaries in which the stellar rotation is synchronized with the orbital motion. Here we consider different stellar models with coalescence times of 1 or 10 Gyr. The top panels show effective spin parameters in logarithmic scales. The bottom panel shows effective spin parameter ranging from  $-0.3$  to  $1$ . Here we assume the mass ratio of binaries is unity for the models. When comparing the models with the data in the bottom panels, we also assume that the BBH spin axes are aligned to the orbital axis. The data are taken from Abbott et al. (2016b).

2011):

$$t_b \approx 15 \text{ s} \left( \frac{L_{j,\text{iso}}}{10^{51} \text{ erg s}^{-1}} \right)^{-1/3} \left( \frac{\theta_j}{10^\circ} \right)^{2/3} \times \left( \frac{R_*}{5R_\odot} \right)^{2/3} \left( \frac{M_*}{15M_\odot} \right)^{1/3}, \quad (12)$$

where  $L_{j,\text{iso}}$  is the isotropic jet luminosity,  $\theta_j$  is the jet's half opening angle,  $R_*$  and  $M_*$  are the radius and mass of the progenitor. Note that these mass and radius that are inferred from the GRB observations of  $L_{j,\text{iso}}$ ,  $\theta_j$ , and  $t_b$  are consistent with the required properties of the progenitors of BBH mergers.

The spin of the progenitor likely plays an essential role in the production of the GRB emission because the formation of a massive accretion torus around a new-born black hole is required to produce the corresponding high luminosity jets (see, e.g., MacFadyen & Woosley 1999). The specific orbital angular momentum at the inner most stable circular orbit is  $j_{\text{ISCO}} = 2\sqrt{3}$  for Schwarzschild black holes and  $2/\sqrt{3}$  for extreme Kerr black holes. Here the angular momentum is normalized by the mass of the central black hole. The specific angular momentum of a mass element of a rigidly rotating star at a radius  $R$  on the equatorial plane is

$$j(R) = \frac{\Omega R^2}{r_{g,\text{BH}} c} = \frac{\chi_*}{\epsilon} \left( \frac{R}{R_*} \right)^2 \left( \frac{M_*}{M_{\text{BH}}} \right), \quad (13)$$

where  $r_{g,\text{BH}}$  is the gravitational radius of the central black

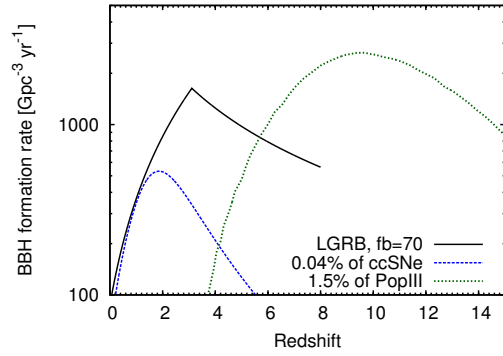


FIG. 3.— The BBH formation rate under the assumptions that it follows (i) the cosmic star formation history, (ii) the LGRB rate, and (iii) the Pop III star formation rate. The BBH formation rates is normalized to be 0.04% of core collapse supernovae for (i; Madau & Dickinson 2014), the LGRB rate with a beaming correction of 70 for (ii; Wanderman & Piran 2010), and 1.5% of Pop III star formation for (iii; de Souza et al. 2011). Here the mean stellar mass of Pop III stars is assumed to be  $20M_\odot$ .

hole and  $\chi_*$  is the dimensionless spin parameter of the star. The condition that the mass elements of the stellar core form an accretion torus is assumed to be  $j(R_c) \geq j_{\text{ISCO}}$  or equivalently:

$$\chi_* \gtrsim 1.3 \left( \frac{\epsilon}{0.075} \right) \left( \frac{R_c}{0.57R_\odot} \right)^{-2} \times \left( \frac{R_*}{1.6R_\odot} \right)^2 \left( \frac{M_{\text{BH}}}{15M_\odot} \right) \left( \frac{M_*}{20M_\odot} \right)^{-1}, \quad (14)$$

where we assume that the central black hole is a Schwarzschild black hole as a conservative choice and  $R_c$  is the stellar core radius<sup>3</sup>. The reference parameters are for a WR star taken from Kushnir et al. (2016). Within this model, LGRBs are produced by black holes only when the progenitor's spin parameter is larger than  $\sim 1.3$ , and thus, the resulting black hole has a large spin (see also Barkov & Komissarov 2010). Using Eq. (6), this condition can be translated to the coalescence time for a given stellar mass as  $t_c \lesssim 0.2 \text{ Gyr } (m/30M_\odot)^{-13/8}$ . Therefore, if the delay-time distribution is roughly  $1/t$  and the minimal coalescence time is  $\sim 10 \text{ Myr}$ , one third of BBH formation with  $t_c < 10 \text{ Gyr}$  have spins which may be large enough to produce LGRBs (see §7 for the delay-time distribution). Note that two LGRBs may lead to a single BBH merger as both the first and the second core collapses may produce GRBs, if they arise from a doubly synchronized system.

## 7. THE SPIN DISTRIBUTION AND ITS REDSHIFT EVOLUTION OF BBH MERGERS

We turn now to the redshift-dependent spin distribution of BBH mergers for different assumptions on the formation rate. We focus on WR progenitors. Here we assume that the spin parameter is  $\chi_{\text{BH}} = \min(\chi_*, 1)$ . We consider two different scenarios: (i) the WR stars are synchronized at the beginning of the WR phase,  $x_{s,i} = 1$ ; (ii) the initial spins of the WR stars are much smaller than the synchronization spin,  $x_{s,i} \approx 0$ . This latter initially low spin case,  $x_{s,i} = 0$ , corresponds to an evolutionary path with a common envelope phase in which the semi-major axis shrinks significantly just prior to the beginning of the WR phase. The spin distribution of BBH mergers can, therefore be used to constrain whether or not a common envelope phase plays an important role for the BBH progenitors.

The BBH merger rate at a given redshift is given by a convolution of the cosmic BBH formation rate and the delay-time distribution. Here we assume a power law distribution of the delay time with a minimal delay time<sup>4</sup>:

$$\frac{dN}{dt_c} = \frac{N_0}{t_c^n} \quad (\text{for } t_c > t_{c,\min}), \quad (15)$$

where the normalization constant  $N_0$  ensures that the integration of Eq. (15) from  $t_{c,\min}$  to a Hubble time is unity and we consider here  $n = 1$  or  $2$  and  $t_{c,\min} = 10 \text{ Myr}$ . Note that this kind of the delay-time distribution is motivated by those of other astrophysical phenomena related to binary mergers. For instance, the delay-time distribution of type Ia supernovae has  $n \approx 1$  and  $t_{c,\min}$  of  $40 \text{ Myr}$  to a few hundreds of Myr (Maoz et al. 2014 and references therein) and that of short GRBs has  $n \approx 1$  and  $t_{c,\min} \approx 20 \text{ Myr}$  (Wanderman & Piran 2010; Ghirlanda et al. 2016).

For the cosmic BBH formation rate, we consider two scenarios: (i) it is proportional to the cosmic star formation rate (SFR; Madau & Dickinson 2014) and (ii) it

<sup>3</sup> If we use as the condition of the disk formation that the mass elements of the core surface have the specific angular momentum of the marginally bound orbit, which is 4 for a Schwarzschild black hole as chosen in Barkov & Komissarov (2010), the critical stellar spin parameter is larger by 15% compared to Eq. (14).

<sup>4</sup> The strong dependence of the merging time on the semi major axis suggest such a distribution with  $n \lesssim 1$ .

equals the LGRBs (Wanderman & Piran 2010). The normalization of the cosmic BBH formation of the LGRB scenario corresponds to the LGRB rate corrected by a beaming factor of  $f_b = 70$ . For the cosmic SFR scenario, our normalization corresponds to one BBH formed every  $2.5 \cdot 10^5 M_\odot$  stellar mass formation. This roughly corresponds to a merging BBH formation rate that is 0.04% of the normal core-collapse supernova rate (assuming that one core collapse supernova occurs every  $100 M_\odot$  stellar mass formation). The cosmic BBH formation rates of these scenarios are shown in Fig. 3.

### 7.1. The spin distribution of BBH mergers in the local Universe

Figure 4 depicts the spin distribution of merging BBHs at  $z = 0.1$ . For simplicity, we consider equal mass binaries. Also shown are the values and upper limits of the spin parameters  $\chi_2$  inferred from LIGO's O1 detections assuming that the spin axes of BBHs are aligned with the orbital axis. We consider two cases relating the effective spin parameters to the component spin  $\chi_2$ : (i) a single synchronization: the primary<sup>5</sup> black hole's spin is negligibly small, i.e.,  $\chi_2 \approx 2\chi_{\text{eff}}$ , and (ii) a double synchronization: the primary black hole is also synchronized with a comparable spin parameter. In this case  $\chi_2 \approx \chi_{\text{eff}}$ .

The spin distribution for  $n = 1$  has two peaks. One is at a high spin  $\chi_2 \sim 1$  and the other is at a low spin  $\chi_2 \sim 0.15$  ( $\ll 0.1$ ) for  $x_{s,i} = 1$  (for  $x_{s,i} = 0$ ). The latter low spin peak corresponds to the spin parameter of BBHs that are formed at the cosmic BBH formation peak. The population is flat between the two peaks. This is simply because of  $dN/d \ln \chi_2 \propto dN/d \ln t_c = \text{const}$ , inferred from Eq. (6). For  $n = 2$ , the population at higher spins ( $\chi_2 \gtrsim 0.3$ ) dominates as expected from the fact that there are more BBHs with shorter coalescence times as  $dN/d \ln \chi_2 \propto \chi_2^{8/3}$  for  $\chi_2 \gtrsim 0.2$ . This feature is irrespective of the assumptions on the initial synchronization parameters and the cosmic BBH formation history. It suggests that a steep delay-time distribution with  $n \gtrsim 2$  is inconsistent with the observed spin distribution. Clearly, given the different assumption, the spin parameter distribution should be between the single synchronization with  $x_{s,i} = 0$  and the double synchronization with  $x_{s,i} = 1$ .

The bimodal spin distribution, that we find, is qualitatively similar to one found by Zaldarriaga et al. (2017). However, the peak at the high spin in our calculation is lower than the one of Zaldarriaga et al. (2017). This is because we use a BBH formation history that peaks at a redshift of 2–3 so that the merger events at the local Universe are dominated by a population with longer coalescence times and therefore they have smaller spins.

### 7.2. The redshift evolution of high/low spin BBH mergers

Figure 5 shows the redshift evolution of the BBH merger rate for the cosmic SFR and the LGRB scenarios. We divide the BBH mergers into two classes (i) high spin ( $\chi_2 > 0.3$ ) and (ii) low spin ( $\chi_2 < 0.3$ ). This threshold spin value corresponds to coalescence times of  $0.3 \text{ Gyr}$

<sup>5</sup> The primary black hole is the one formed at the first core collapse for our definition. It is not necessarily the more massive one.



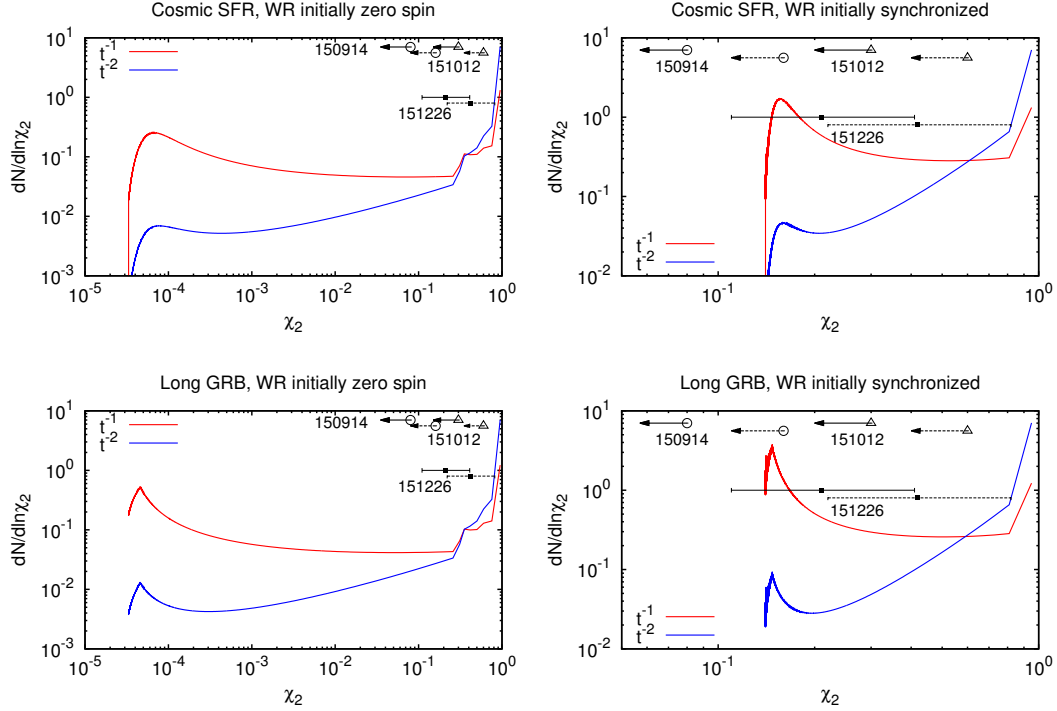


FIG. 4.— The spin distribution of BBH mergers at  $z = 0.1$  for BBH formation history that follows the cosmic star formation history (top panels) and the LGRB rate (bottom panels). The distributions are calculated under the assumptions that the initial spin angular momentum of the WR stars vanishes, i.e.,  $x_{s,i} = 0$  (left) and the WR stars are initially tidally synchronized, i.e.,  $x_{s,i} = 1$  (right). We use two different delay-time distribution  $n = 1$  and  $2$  with a minimal time delay of 10 Myr. We set the mass ratio,  $q$ , to be unity and the total mass to be  $60M_{\odot}$ . The location of the peak at lower spins slightly shifts with changing the masses. Also shown are the  $\chi_2$  values inferred from the LIGO’s O1 three detections. The measured effective spin parameters are translated to  $\chi_2$  assuming  $\chi_1 = \chi_2$  (solid line and arrows) and  $\chi_1 = 0$ . Here we assume that the BBH spin axes are aligned with the orbital axis hence we show the upper limits on the spin parameters of GW150914 and LVT151004. Note that the measured spin parameters of these BBHs can be negative (see Table 1).

and 1.5 Gyr for  $x_{s,i} = 0$  and  $x_{s,i} = 1$ , respectively. Because of the longer delay of the lower spin population the high spin BBH mergers predominately occur at higher redshifts. In all cases, the merger rate of the low spin population is larger than that of the high spin one in the local Universe. An interesting feature is that the merger rate of the high spin population starts to dominate over the low spin one at a redshift of  $\sim 0.5$ – $1.5$ . Mergers at such redshifts could be detected by upgraded GW detectors in future.

The BBH merger history, which is a convolution of the formation history with a delay-time distribution, is not very sensitive to the assumption of the BBH formation history, i.e., LGRB or cosmic star formation history, as long as the latter peaks around a redshift of 2–3.

To produce LGRBs, the black holes should have extreme spins (see §6). This is not the case for LIGO’s O1 detections<sup>6</sup>. However, as noted earlier, BBHs with high spins have short merger times thereby we do not observe most of these mergers in the local Universe. If the delay-time distribution is  $\sim 1/t$  with  $t_{\min} = 10$  Myr, we expect that the current event rate of BBH mergers with extreme spins is  $\leq 20\%$  of the total merger rate. The corresponding high spin BBH merger rate is

$\lesssim 20^{+28}_{-14} \text{ Gpc}^{-3} \text{ yr}^{-1}$ . On the other hand, the local rate of LGRBs is  $\sim 91^{+42}_{-49} \text{ Gpc}^{-3} \text{ yr}^{-1} (f_b/70)$ , where  $f_b$  is a beaming correction factor (Wanderman & Piran 2010). Note that the LGRB rate should be compared with twice of the high spin BBH merger rate for the double synchronization case. These rates are consistent with each other within the admittedly large uncertainties. This suggests that it is possible that the two phenomena share same progenitors.

### 7.3. Pop III BBH mergers

Figure 6 shows the redshift evolution of BBH mergers for the Pop III scenario. Here we use a Pop III star formation rate derived by de Souza et al. (2011)<sup>7</sup>. We normalize the Pop III BBH formation rate such that 1.5% of Population III stars form BBHs with coalescence times less than a Hubble time (Inayoshi et al. 2017). Here we assume a mean stellar mass of  $20M_{\odot}$ , a delay-time distribution with  $n = 1$  and a minimal time delay of 0.4 Gyr. This minimal time delay roughly corresponds to the minimal semi-major axis for which the radius of Pop III main-sequence stars is smaller than the Roche limit.

<sup>6</sup> Unless the spin-orbit misalignments are significant. Note also that the observed  $\chi_{\text{eff}}$  of GW151226 does not rule out the possibility that the less massive black hole has a spin parameter of order unity.

<sup>7</sup> This Pop III star formation rate seems the maximum allowed by the Planck observations of the electron scattering opacity to the cosmic microwave background within two  $\sigma$  (see, e.g., Visbal et al. 2015 for details).



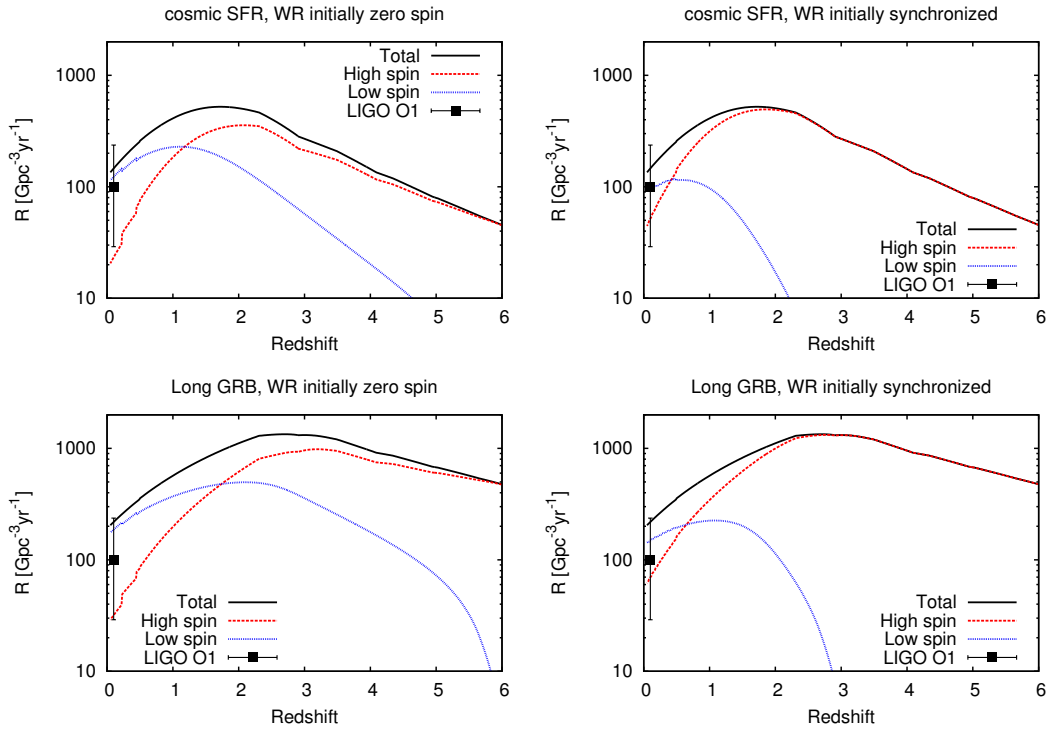


FIG. 5.— The redshift evolution of BBH mergers for the cases that the BBH formation follows the cosmic star formation history (top panels) and the LGRB rate (bottom panels). We separate the mergers into the high and low spin populations with a threshold spin of  $\chi_2 = 0.3$ . Here we assume a delay-time distribution with  $n = 1$  and a minimal time delay of 10 Myr. The total merger rate in the local Universe estimated by Abbott et al. (2016b) is shown as a square.

The redshift evolution of Pop III BBH mergers is significantly different from other astrophysical scenarios. It increases up to  $z \sim 5$ , which is beyond the peaks of the cosmic star formation history and the LGRB rate. This by itself can be used to distinguish this scenario from the others (see also Nakamura et al. 2016). Another prediction of this scenario is that the spin parameters of BBH mergers at higher redshifts above  $\sim 4-5$  may be dominated by an extreme spin population with  $\chi_2 \sim 1$ . Clearly, significant improvements in GW detectors is needed to detect such events.

## 8. CAVEATS

*Uncertainties in the synchronization:* The tidal synchronization relevant to the BBH progenitors is due to dynamical tides that are excited above the convective core and dissipate in the radiative envelope (Zahn 1975; Goldreich & Nicholson 1989; Kushnir et al. 2017). Once a stellar structure is given, one can calculate the tidal torque on the star. However, massive stellar envelopes might be turbulent and unstable. In such cases, synchronization due to an equilibrium tide in the envelope can be more efficient (see, e.g., Toledano et al. 2007; Detmers et al. 2008). In this case the synchronization time behaves as  $\propto q^{-2}(a/R)^6$ . This additional effect will speed up the synchronization. Note also that we have assumed circular orbits in this paper. One should use estimates of the synchronization time including resonant excitations of g-modes when considering elliptic orbits (Witte & Savonije 1999). But these effects are beyond the scope of this paper. We will address this issue in a separate work.

The angular momentum loss due to winds is uncertain and it depends on the stellar metallicities. While our results depend on the wind strength, the qualitative results in this paper are robust. Indeed, Zaldarriaga et al. (2017) show the robustness of this spin argument for WR progenitors for different wind parameters.

*Mass loss and natal kick at the core collapse:* We have assumed here that the mass of black holes is identical to that of the collapsing stars. This assumption is likely valid as long as the spin parameter of the progenitors does not exceed unity (Sekiguchi & Shibata 2011; O’Connor & Ott 2011). When the progenitor’s spin exceeds unity, a fraction of the progenitor’s mass is ejected carrying the excess angular momentum, and hence, the black hole has a mass smaller than the progenitor’s mass (Barkov & Komissarov 2010). For WR stars, this effect is expected to be small since their maximal spin parameter does not significantly exceed unity.

One of the major concerns about the spin argument is that it is assumed that the direction of the spin angular momentum is parallel to the orbital angular momentum. This assumption is crucial because GW measurements are insensitive to the spin parameters perpendicular to the orbital angular momentum. The tidal torque always works toward the orientation of the stellar spins to be parallel to the orbital angular momentum. Other effects of the binary interaction, e.g., mass transfer, also change the spin components parallel to the orbital angular momentum. It has been suggested that the progenitor receives a natal kick during the core collapse (e.g. Janka 2013). This may cause a misalignment between

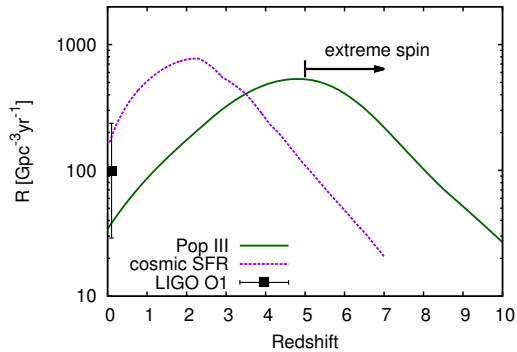


FIG. 6.— The same as Fig. 5 but for the Pop III scenario. Also shown is the redshift evolution of the cosmic SFR scenario for a comparison. An arrow depicts the redshift where BBH mergers with extreme spins start to dominate the event rate.

the spin axes and the orbital axis. However, to significantly change the direction of the orbital angular momentum one needs a kick  $\gtrsim 500$  km/s. While such kicks have been observed at the high end of pulsar kicks we do not expect such large natal kicks during black holes formation. The fraction of the ejected mass to the remnant mass in this case is expected to be much smaller for black hole formation than the ratio in neutron star formation (see Janka 2013 and also Rodriguez et al. 2016b for a detailed study of the distributions  $\chi_{\text{eff}}$  including the natal kicks). Furthermore, observations of low mass X-ray binaries show no evidence of strong natal kicks of black holes (see, e.g., Mandel 2016). These suggest typical values that are much smaller than the orbital velocities of the BBH progenitors. Therefore, we expect that BBH natal kicks may not affect significantly the spin components parallel to the orbital axis of the black holes and hence the results of our analysis (see also discussions in Abbott et al. 2016a).

*Mass transfer and Common envelope phases:* We considered two scenarios, (i) single synchronization and (ii) double synchronization. The spin of the black hole formed at the second core collapse of a binary is conserved as long as there is no significant mass accretion from the interstellar medium. Therefore, the spin parameters in the single synchronization case may be quite robust. On the contrary, the spin of the black hole formed at the first core collapse can change from the value at the birth of the black hole due to the mass accretion from the companion. Moreover, the semi-major axis may further change after the first core collapse due to a common envelope phase. If this occurs, the spin parameter of this black hole has nothing to do with the initial semi-major axis of BBHs. Thus, the double synchronization case involves some uncertainties, or equivalently, the spin parameter of one of the black holes in BBH mergers is not well constrained by the tidal synchronization argument.

*Spin reduction due to the Blandford-Znajek process:* One of the possible mechanisms powering GRB central engines is the Blandford-Znajek process, in which the rotational energy of a central black hole is removed through magnetic fields and an ultra-relativistic jet is launched with this energy (Blandford & Znajek 1977). While we still don't know whether or not this process works in collapsing massive stars and what the back reaction of this

process on the central black hole is, if this process removes a significant amount of the rotational energy, the spin of the black hole is reduced.

## 9. CONCLUSIONS

The spins (projected on the orbital angular momentum axis) of the merging black holes observed by LIGO O1 run are rather small. We have examined the implications of these observations on the progenitor scenarios in which BBHs arise from isolated field binaries. Our analysis was done under the assumption that this projection indeed reflects the final spin of the progenitor star, just before it collapsed to a black hole. As the expected mass ejected during the formation of the black hole is rather small compared with the remnant black hole we do not expect a strong natal kick and hence a significant change in the black hole's spin or in the orbital angular momentum (see Rodriguez et al. 2016b for the effects of natal kicks on the effective spin parameters).

We have studied the spin distribution and its redshift evolution based on the tidal synchronization argument (Kushnir et al. 2016). We find that massive main-sequence progenitors, whose semi-major axis is small enough to merge within a Hubble time, the tidal synchronization occurs on timescales much shorter than their lifetime. As a result, the spin parameters of such main-sequence stars exceed unity. Given the fact that the aligned spin parameters of the three LIGO's O1 events measured via the GW signals are significantly less than unity, we can rule out the possibility that these BBHs are formed directly from the collapse of main-sequence stars. This also indicates that, if the BBHs formed via binary evolution beginning with two main-sequence stars, the progenitor binary systems must experience either a significant loss of their spin angular momentum (more than 95%) or a significant decrease in the semi-major axis during their evolution. This conclusion is consistent with current stellar and binary evolution studies (see, e.g., Belczynski et al. 2016).

Among known stellar objects, WR stars seem to be the only possible progenitors of the BBH mergers. We consider the spin distribution and redshift evolution of BBH mergers formed via WR progenitors, taking the synchronization, mass loss, and stellar lifetime, into account. Here we assume that the cosmic BBH formation history is proportional to either the cosmic SFR or to LGRB rate (LGRBs are also formed from WR stars) with two different delay-time distributions. We find that a steep delay-time distribution  $\propto 1/t^2$  predicts too many BBH mergers with extreme spins  $\chi \sim 1$ . This is inconsistent with the LIGO's O1 events. On the contrary, for the delay-time distribution of  $\propto 1/t$ , the rate of BBH mergers with low spins ( $\chi \lesssim 0.3$ ) dominates over the one with high spins ( $\chi \gtrsim 0.3$ ) in the local Universe. The ratio of the high spin mergers to the low ones increases with the cosmological redshift and the high spin population begins to dominate at a redshift of 0.5–1.5. This feature may be observable by GW detectors network in future.

The BBH merger rate density inferred from LIGO's O1 run is compatible with that of LGRBs. Motivated by this, we considered the possibility that BBH mergers and LGRBs share the same progenitors, i.e, LGRBs are produced at the core collapse of stars in a close binary which eventually evolves to a BBH with a coalescence

time of less than a Hubble time. We show that a stellar spin parameter of  $\gtrsim 1.3$ , or equivalently a coalescence time of  $\lesssim 0.2$  Gyr, is required for WR progenitors in order that a fraction of the stellar core forms an accretion disk around the central black hole. Assuming a delay-time distribution of  $1/t$  with the minimal delay-time of 10 Myr, we expect that the LGRB rate is about one third of the BBH formation rate. Because BBHs with such extreme spins predominately merge at high redshifts, it is still possible that BBH mergers and LGRBs share the same progenitors even though the aligned spin parameters of the LIGO's O1 events are significantly less than unity. We extrapolate the total BBH merger rate with low spins inferred from LIGO's O1 run to the extreme spin population based on the WR progenitor scenario and show that the BBH merger rate with extreme spins is 20% of the total rate or less. This can be tested in the near future with further observations of BBH mergers.

We also considered the hypothetical Pop III BBH merger scenario. As these BBHs formed at high redshifts around  $z \sim 10$ , in the local Universe, BBH mergers from Pop III stars always have a time delay of  $\sim 10$  Gyr. If they arise from synchronized stars, this corresponds to the BBH spin parameters of 0.2–0.6. However, it is not clear that these Pop III binaries are fully synchronized during their main-sequence phase as the synchronization time is comparable to their lifetime. Furthermore, a fraction of the spin angular momentum may be removed during the stable mass transfer in the late phases and this may reduce the spin parameters (see Inayoshi et al. 2017). Therefore we conclude that the Pop III star sce-

nario can be consistent with the low aligned spins of the three LIGO's O1 events. In this scenario the BBH merger rate increases with the redshift up to  $z \sim 5$  and we expect BBH merges with extreme spins beyond a redshift of 4. These are unique observable features of this scenario.

To summarize, we have shown that the low aligned spins of the BBH mergers observed in LIGO's O1 run are consistent with WR progenitors. Those are also progenitors of LGRBs and given the comparable observed rate it might be that LGRBs arise when the WR progenitors collapse to form the observed BBHs. While the observed spins are slightly lower than expected, Pop III stars cannot be ruled out either. Both scenarios predict that some high aligned spin BBHs should be discovered as well. If these are not discovered within LIGO's coming runs, then the observations will imply that it is unlikely that LIGO's BBHs have been formed via regular binary stellar evolution channels, and then, the capture in dense environments (clusters or galactic cores) or primordial origin will be preferred.

We thank Maxim Barkov, Matteo Cantiello, Sivan Ginzburg, James Guillochon, Kohei Inayoshi, Tomoya Kinugawa, Itai Linial, Masaru Shibata, Maurice van Putten, and Roni Waldman for useful discussions and comments. KH is supported by the Flatiron Fellowship at the Simons Foundation. The research was supported by an advanced ERC grant TRex and by the ISF-CHE I-Core center of excellence for research in Astrophysics.

## REFERENCES

- Abbott, B. P., et al. 2016a, *ApJ*, 818, L22  
—, 2016b, *Physical Review X*, 6, 041015  
—, 2016c, *Physical Review Letters*, 116, 061102  
Antonini, F., & Rasio, F. A. 2016, *ApJ*, 831, 187  
Barkov, M. V., & Komissarov, S. S. 2010, *MNRAS*, 401, 1644  
Bartos, I., Kocsis, B., Haiman, Z., & Márka, S. 2017, *ApJ*, 835, 165  
Belczynski, K., Holz, D. E., Bulik, T., & O'Shaughnessy, R. 2016, *Nature*, 534, 512  
Bird, S., Cholis, I., Muñoz, J. B., Ali-Haïmoud, Y., Kamionkowski, M., Kovetz, E. D., Raccanelli, A., & Riess, A. G. 2016, *Physical Review Letters*, 116, 201301  
Blandford, R. D., & Znajek, R. L. 1977, *MNRAS*, 179, 433  
Blinnikov, S., Dolgov, A., Porayko, N. K., & Postnov, K. 2016, *JCAP*, 11, 036  
Bromberg, O., Nakar, E., Piran, T., & Sari, R. 2011, *ApJ*, 740, 100  
—, 2012, *ApJ*, 749, 110  
Bulik, T., Belczynski, K., & Prestwich, A. 2011, *ApJ*, 730, 140  
Carpano, S., Pollock, A. M. T., Prestwich, A., Crowther, P., Wilms, J., Yungelson, L., & Ehle, M. 2007, *A&A*, 466, L17  
Crowther, P. A., Barnard, R., Carpano, S., Clark, J. S., Dhillon, V. S., & Pollock, A. M. T. 2010, *MNRAS*, 403, L41  
de Souza, R. S., Yoshida, N., & Ioka, K. 2011, *A&A*, 533, A32  
Detmers, R. G., Langer, N., Podsiadlowski, P., & Izzard, R. G. 2008, *A&A*, 484, 831  
Eggleton, P. P. 1983, *ApJ*, 268, 368  
Esposito, P., Israel, G. L., Milisavljevic, D., Mapelli, M., Zampieri, L., Sidoli, L., Fabbiano, G., & Rodríguez Castillo, G. A. 2015, *MNRAS*, 452, 1112  
Farr, W. M., Sravan, N., Cantrell, A., Kreidberg, L., Bailyn, C. D., Mandel, I., & Kalogera, V. 2011, *ApJ*, 741, 103  
Ghirlanda, G., et al. 2016, *A&A*, 594, A84  
Goldreich, P., & Nicholson, P. D. 1989, *ApJ*, 342, 1079  
Hirano, S., Hosokawa, T., Yoshida, N., Umeda, H., Omukai, K., Chiaki, G., & Yorke, H. W. 2014, *ApJ*, 781, 60  
Hirschi, R., Meynet, G., & Maeder, A. 2004, *A&A*, 425, 649  
Hosokawa, T., Omukai, K., Yoshida, N., & Yorke, H. W. 2011, *Science*, 334, 1250  
Hurley, J. R., Pols, O. R., & Tout, C. A. 2000, *MNRAS*, 315, 543  
Inayoshi, K., Hirai, R., Kinugawa, T., & Hotokezaka, K. 2017, *ArXiv e-prints*  
Ivanova, N., et al. 2013, *A&A Rev.*, 21, 59  
Janka, H.-T. 2013, *MNRAS*, 434, 1355  
Kashlinsky, A. 2016, *ApJ*, 823, L25  
Kinugawa, T., Inayoshi, K., Hotokezaka, K., Nakauchi, D., & Nakamura, T. 2014, *MNRAS*, 442, 2963  
Kruckow, M. U., Tauris, T. M., Langer, N., Szécsi, D., Marchant, P., & Podsiadlowski, P. 2016, *A&A*, 596, A58  
Kushnir, D., Zaldarriaga, M., Kollmeier, J. A., & Waldman, R. 2016, *MNRAS*, 462, 844  
—, 2017, *MNRAS*, 467, 2146  
Langer, N., Hamann, W.-R., Lennon, M., Najarro, F., Pauldrach, A. W. A., & Puls, J. 1994, *A&A*, 290, 819  
Liu, J.-F., Bregman, J. N., Bai, Y., Justham, S., & Crowther, P. 2013, *Nature*, 503, 500  
MacFadyen, A. I., & Woosley, S. E. 1999, *ApJ*, 524, 262  
Madau, P., & Dickinson, M. 2014, *ARA&A*, 52, 415  
Mandel, I. 2016, *MNRAS*, 456, 578  
Mandel, I., & de Mink, S. E. 2016, *MNRAS*, 458, 2634  
Maoz, D., Mannucci, F., & Nelemans, G. 2014, *ARA&A*, 52, 107  
Marchant, P., Langer, N., Podsiadlowski, P., Tauris, T. M., & Moriya, T. J. 2016, *A&A*, 588, A50  
Marigo, P., Girardi, L., Chiosi, C., & Wood, P. R. 2001, *A&A*, 371, 152  
Meynet, G., Georgy, C., Hirschi, R., Maeder, A., Massey, P., Przybilla, N., & Nieva, M.-F. 2011, *Bulletin de la Societe Royale des Sciences de Liege*, 80, 266  
Meynet, G., & Maeder, A. 2003, *A&A*, 404, 975  
—, 2005, *A&A*, 429, 581  
—, 2007, *A&A*, 464, L11  
Nakamura, T., et al. 2016, *Progress of Theoretical and Experimental Physics*, 2016, 093E01  
O'Connor, E., & Ott, C. D. 2011, *ApJ*, 730, 70  
O'Leary, R. M., Meiron, Y., & Kocsis, B. 2016, *ApJ*, 824, L12  
Omukai, K., & Palla, F. 2003, *ApJ*, 589, 677  
Özel, F., Psaltis, D., Narayan, R., & McClintock, J. E. 2010, *ApJ*, 725, 1918  
Peters, P. C. 1964, *Physical Review*, 136, 1224  
Podsiadlowski, P., Mazzali, P. A., Nomoto, K., Lazzati, D., & Cappellaro, E. 2004, *ApJ*, 607, L17  
Prestwich, A. H., et al. 2007, *ApJ*, 669, L21  
Ramírez-Agudelo, O. H., et al. 2015, *A&A*, 580, A92

- Rodriguez, C. L., Haster, C.-J., Chatterjee, S., Kalogera, V., & Rasio, F. A. 2016a, *ApJ*, 824, L8
- Rodriguez, C. L., Zevin, M., Pankow, C., Kalogera, V., & Rasio, F. A. 2016b, *ApJ*, 832, L2
- Sasaki, M., Suyama, T., Tanaka, T., & Yokoyama, S. 2016, *Physical Review Letters*, 117, 061101
- Sekiguchi, Y., & Shibata, M. 2011, *ApJ*, 737, 6
- Silverman, J. M., & Filippenko, A. V. 2008, *ApJ*, 678, L17
- Stone, N. C., Metzger, B. D., & Haiman, Z. 2017, *MNRAS*, 464, 946
- Toledano, O., Moreno, E., Koenigsberger, G., Detmers, R., & Langer, N. 2007, *A&A*, 461, 1057
- Tout, C. A., Pols, O. R., Eggleton, P. P., & Han, Z. 1996, *MNRAS*, 281, 257
- Ud-Doula, A., Owocki, S. P., & Townsend, R. H. D. 2009, *MNRAS*, 392, 1022
- van den Heuvel, E. P. J., Portegies Zwart, S. F., & de Mink, S. E. 2017, *ArXiv e-prints*
- Visbal, E., Haiman, Z., & Bryan, G. L. 2015, *MNRAS*, 453, 4456
- Wanderman, D., & Piran, T. 2010, *MNRAS*, 406, 1944
- Witte, M. G., & Savonije, G. J. 1999, *A&A*, 350, 129
- Woosley, S. E. 1993, *ApJ*, 405, 273
- Woosley, S. E., & Heger, A. 2012, *ApJ*, 752, 32
- Zahn, J.-P. 1975, *A&A*, 41, 329
- . 1977, *A&A*, 57, 383
- Zaldarriaga, M., Kushnir, D., & Kollmeier, J. A. 2017, *ArXiv e-prints*